ChemComm

HIGHLIGHT

View Article Online
View Journal | View Issue

Cite this: *Chem. Commun.*, 2023, **59**, 10464

The rise of metal–organic framework based micromotors

Javier Bujalance-Fernández, [a] Beatriz Jurado-Sánchez *[ab] and Alberto Escarpa *[ab]

Micromotors (MMs) are micro and nanoscale devices capable of converting energy into autonomous motion. Metal–organic frameworks (MOFs) are crystalline materials that display exceptional properties such as high porosity, internal surface areas, and high biocompatibility. As such, MOFs have been used as active materials or building blocks for MMs. In this highlight, we describe the evolution of MOF-based MMs, focusing on the last 3 years. First, we covered the main propulsion mechanisms and designs, from catalytic to fuel-free MOF-based MMs. Secondly, we discuss recent applications of new fuel-free MOFs MM to give a critical overview of the current challenges of this blooming research field. The advantages and challenges discussed provide a useful guide for the design of the next generation MOF MMs toward real-world applications.

Received 8th June 2023,
Accepted 1st August 2023

DOI: 10.1039/d3cc02775a

rsc.li/chemcomm

1. Introduction: some basic aspects of metal–organic frameworks and micromotors

MOFs are crystalline materials with a periodic network of organic ligand linkers bonded with metal ion nodes to create one, two or three-dimensional structures (see the general structure of MOFs in Scheme 1). MOFs display exceptional properties such as high porosity, internal surface areas of up

[a] *Department of Analytical Chemistry, Physical Chemistry and Chemical Engineering, University of Alcala, Alcala de Henares, Madrid, E-28871, Spain. E-mail: beatriz.jurado@uah.es, alberto.escarpa@uah.es; Tel: +34 91 8854995*
[b] *Chemical Research Institute "Andres M. del Rio", University of Alcala, Alcala de Henares, Madrid, E-28871, Spain*

Javier Bujalance-Fernández

Javier Bujalance Fernández received a BSc (2018) in biology from the University of Córdoba, Spain. He received a MSc in Health Biology at Complutense University in 2020. In 2021, he started his PhD, thanks to a grant, at the University of Alcalá focusing on biomedical applications of metal–organic frameworks under the supervision of Professor Beatriz Jurado and Professor Alberto Escarpa.

Beatriz Jurado-Sánchez

Beatriz Jurado Sánchez is Associate Professor at the University of Alcalá. Her research interests are the synthesis of tubular and Janus micromotors based on nanomaterials, the integration of micromotors into portable instrumentation, biosensing with micromotors integrating quantum dots, and the development of micromotor-based environmental remediation approaches. Prof. Jurado has co-authored over 82 scientific papers (H Index = 37), 5 book chapters, and more than 20 communications at international conferences. Her research has been highlighted as a cover in the top impact journals Angewandte Chemie International Edition, Chemical Science, and Analytical Chemistry. She is currently Associate Editor at RSC Advances.

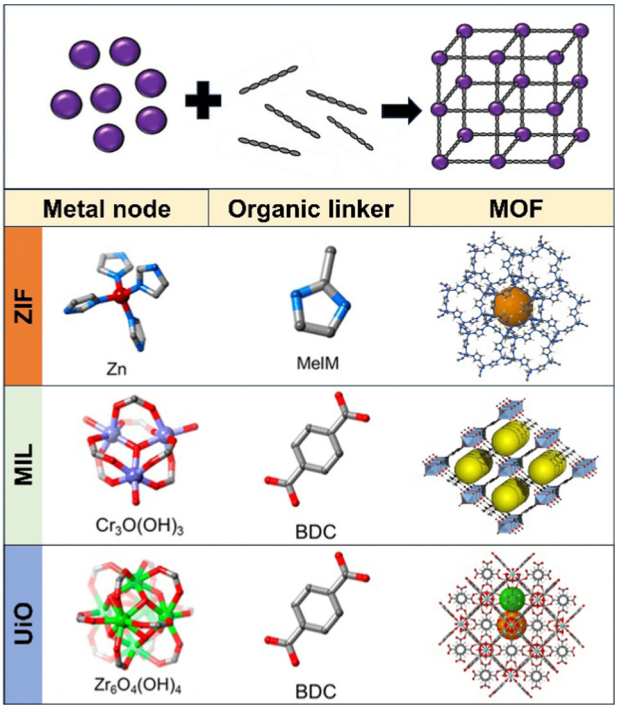

Scheme 1 Schematic of the general structure of MOFs and representative metal nodes, organic ligands, and crystal structures of ZIF, MIL and UiO MOFs. Reproduced from ref. 23 with permission from Wiley, copyright 2018 and from ref. 24 with permission from American Chemical Society, copyright 2017.

to 6 000 m^2 g^{-1} and high biocompatibility.[1–3] There are many ways to classify MOFs into different subtypes, if we look at their component unit, they could be grouped into dozens of subtypes, among them, we can highlight the following: (i) zeolitic imidazolate framework (ZIF), (ii) Materials Institute Lavoisier (MIL) and (iii) University of Oslo (UiO).[4–7] As can be seen in Scheme 1, ZIF MOFs contain tetrahedrally coordinated metal nodes (divalent cations such as Zn^{2+} and Fe^{2+}) bonded to 4 imidazolate groups (MeIM) in a three-dimensional network. The metal–ligand bond possesses a dihedral angle of 145°, like zeolites, but with neutral charges and larger void spaces for ligand exchange/storage.[8,9] In the case of MIL, the metal is a trivalent cation (such as Cr^{3+}) interconnected by 1,4-benzenedicarboxylates (BDCs) into octahedral clusters. This results in a highly porous 3-dimensional structure with large pores suitable for functionalization or guest encapsulation. The Cr metal also possesses catalytic activity.[10] UiO-type MOFs are based on $Zr_6O_4(OH)_4$ octahedra as metal nodes that form lattices by 12-fold connection BDC linkers. Since each Zr octahedron is 12-fold connected to adjacent octahedra, the structure is highly stable to temperatures, degradation, *etc.*[11]

The myriad of available designs and versatility of MOF synthesis, along with the exceptional properties have resulted in many applications in diverse fields such as gas storage or energy generation,[12,13] pollutant removal,[14] analytical biosensing,[15,16]drug delivery,[17] among others.[18] Since the discovery of MOFs in the 1990s, this field has been one of the most studied topics in the current scientific scenario.[7,19,20] A promising research direction, scarcely explored to date, is the marriage of MOFs with self-propelled MMs.[21,22]

MMs are microscale devices capable of converting energy into autonomous motion in a solution.[25,26] From early reports in 2004 to date,[25,27] this blooming field has evolved from achieving propulsion to unprecedented applications such as *in vivo* sensing,[28] on-body treatment of bacterial infections[29] or thrombus therapy.[30] The potential of MMs in such fields is based on the autonomous self-propulsion in confined environments and microvolumes of samples. Indeed, the enhanced fluid mixing and motion of MMs accelerated greatly the kinetics of a reaction or allowed for localized drug delivery.[31,32] A key issue, and at the same time the drawback of the applications of MMs, is their biocompatibility, in terms of propulsion mechanisms and materials.

Catalytic MMs compromise tubular MMs prepared either by electrodeposition routes[33,34] or rolled-up technology.[35,36] Such configurations display an outer polymeric or nanomaterial-based layer and an inner catalytic layer (Pt, Ag, and MnO_2) for propulsion using hydrogen peroxide (H_2O_2) as "fuel". The catalytic reaction takes place in the inner layer, resulting in the ejection of oxygen gas for efficient propulsion in solution. Catalytic Janus MMs compromise polystyrene microspheres half-covered with a metallic layer (normally, Pt) by chemical vapor deposition or oil-in-water emulsion approaches.[37,38] Such asymmetric structure allows for localized oxygen gas production for efficient propulsion. Additionally, magnetic Ni or ferrite layers can be included in the structure for external propulsion control.[39] Fuel free-schemes compromise ultrasound, magnetic or light-driven MMs.[40] Different sizes and shapes have been proposed to achieve directional propulsion, including concave rod shape[41,42] or red-blood cells half-decorated with iron oxide for ultrasound propulsion,[43] magnetic helices or magnetic nanoparticles containing MMs for magnetic propulsion[44,45] and Janus-like type particles or MMs

Alberto Escarpa

Alberto Escarpa is a Full Professor at the University of Alcalá. His main research interests are focused on microfluidics and micromotors. He has co-authored more than 200 articles in leading international peer-reviewed journals, and several books, and book chapters. He has given several invited lectures in prestigious forums. He has been included in Stanford University's list of the 2% of the most cited scientists. His research has been highlighted as cover in Angewandte Chemie, Chemical Science, Nanoscale, and Analytical Chemistry. He is a member of the Editorial Advisory Board of Analytical Chemistry. He is Editor in Chief for Microchimica Acta.

composed of photoactive materials for light-driven propulsion.[46,47] Indeed, controlling the geometry and composition of colloidal particles is a convenient mean to control the light-responsive behaviour, controlled bending, assembly, *etc.*[48,49] Similarly, the structure and composition of MOFs can be controlled to achieve similar features in MM design. For example, MIL-96 MOFs can be prepared in different sizes and shapes by using different solvents and modulators.[50] Acoustomicrofluidic technology has been used to tailor the synthesis of Cu based MOFs, controlling the exposition of the active metal site on demand, which can be further exploited to tailor the catalytic performance of MMs based on MOFs.[51]

Materials aspects also play an important role in the propulsion and applications of MMs. Indeed, the combination of MMs with polymers,[37,52] carbon nanomaterials,[34,53] transition-metal dichalcogenides,[54,55] MXenes,[56] photoactive materials,[56] *etc.*, have resulted in synergetic units with enhancing propulsion and capabilities in a myriad of applications. In this context, the combination of MOFs with MMs can result in a synergetic technology benefiting both from the enhanced fluid mixing of MMs and the exceptional properties of MOFs such as the capability for drug or probes encapsulation, *etc.* The first report of MOF based motion was done by Matsui *et al.* in 2012, who encapsulated diphenylalanine in Cu-JAST based MOFs for Marangoni based-propulsion.[57] Later, in 2014 and 2017, catalytic MOFs propulsion was illustrated by pioneering groups in the field.[58,59] Since then, the field has evolved to the design of fuel-free MOF schemes in a myriad of applications. Two excellent previous reviews from Pumera's and Pané's groups in early 2020 covered the progress so far in the design of MOF based MMs.[21,22] While still in early infancy, the field of MOF based MMs has evolved since then into sophisticated designs and efficient applications in the environmental, biomedical and analytical fields. The aim of these highlights is to critically discuss and establish the advantages, disadvantages and prospects of MOF based MMs in diverse fields, with a special focus on the vast development in the past 3 years (2020 to 2023). We will describe first the evolution of the propulsion and the different MOFs used for biocompatible and fuel-free MM design. Secondly, we will cover recent applications of the new fuel-free configurations, to finally give a critical overview of the current challenges of this blooming research field.

2. Material aspects and evolution of MOF micromotors: from catalytic to fuel-free schemes

Fig. 1 shows a schematic of the evolution of MOF based MMs in terms of propulsion. As can be seen, the type of propulsion (catalytic or fuel-free) has a strong influence on the given application. Catalytic designs can be used in analytical applications, especially for *in vitro* detection. On the contrary, for biomedical applications, fuel-free configurations are desired to avoid cell damage by H_2O_2. Environmental applications lie in the middle point, as in some cases H_2O_2 is used as a co-reagent in many degradation processes. Another obvious trend reflected in Fig. 1 is the quest for full biocompatible MOF MMs, in line with recent trends in the field. As can be also seen, MOFs explored for MMs preparation are ZIF, MIL and UiO material types. This section will be organized according to the catalytic and fuel-free mechanism and to help the reader, Fig. 2 shows a schematic of the general propulsion mechanism.

2.1 First steps: chemical and catalytic propulsion

The first moving MOF MM was propelled by the Marangoni-based effect, which consisted of the creation of a liquid flow due to the generation of local gradients by *i.e.*, the release of a surfactant. This induces an asymmetry in the surface tension, resulting in motion.[60–62] In this context, the high surface area of MOFs and the presence of free sites for molecules encapsulation, allow for the design of such first Marangoni-moving MOFs. The design consisted of a Cu^{2+}-1,4-benzenedicarboxylate-triethylenediamine MOF as a host for diphenylalanine (DPA) peptides, which act as active elements for the Marangoni propulsion. In the presence of sodium ethylenediaminetetraacetate, the MOF structure is partially destructed, releasing DPA in the media. This creates a surface tension gradient and the MM moves to the higher surface tension areas.[57] Later on, the authors illustrated the intelligent chemotactic behavior of the system for pH sensing by combination with enzymes and PbSe quantum dots.[63]

The next logical step, following the general trend in the field, was the design of bubble (or catalytic) propelled MOF MMs as an intermediate step towards fuel-free design. The first work was reported by Chin *et al.* in 2014. A Janus MM structure was designed by asymmetrically coating ZIF-8 MOFs with ZIF-67 containing cobalt as the catalytic metal. Such asymmetric structure allows the MMs propulsion at speeds of up to 1000 μm s^{-1} in 10% H_2O_2 solutions.[58] Asymmetric modification of ZIF-8, UiO-66 or UiO-66-SH MOFs with metals such as Au and Pt have been also reported by using sputter deposition. To this end, the MOFs are dispersed as a monolayer in solid support, with half of the surface protected and the other half exposed for subsequent metal deposition. The Pt containing MOFs results in efficient catalytic MMs for propulsion at speeds of over 1500 μm s^{-1} in 20% H_2O_2 solutions.[67] Such smart designs benefit from the extraordinary properties of MOFs, such as the capability of the introduction of catalytic metals in the structure and controlled nucleation for the creation of optimal structures for efficient and directional motion. Later, Wang's group illustrated the motion of catalytic MOF MMs with built-in engines integrated into the structure. Thus, Zr based UiO-67 bipyridine type MOFs were used as multifunctional units due to their tunability in terms of catalyst metal site design. The MOF platform was mixed with 2,2′-bipyridine-dicarboxylic and biphenyldicarboxylic acids as connecting ligands. This allows for the metalation of the resulting active sites with cobalt or manganese as catalytic metals. The resulting MMs reach speeds of up to 60 μm s^{-1} in the presence of 15% H_2O_2. Interestingly, the use of chelators such as ethylenediaminetetraacetic acid allows the control of the speed and

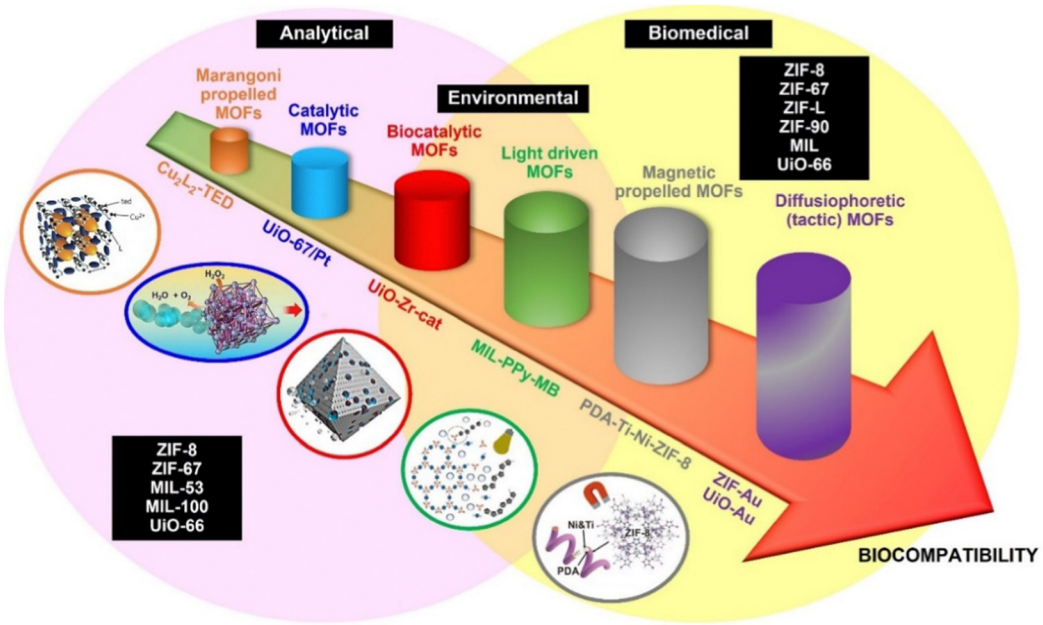

Fig. 1 Schematic of the evolution of MOF MM propulsion, main applications and materials used from their preparation. Bottom images show representative pictures of each design and are reproduced (from top to bottom) from ref. 57 with permission from Nature, copyright 2012; ref. 59 with permission from American Chemical Society, copyright 2017; ref. 64 with permission from American Chemical Society, copyright 2020; ref. 65 with permission from Wiley, Copyright 2022 and ref. 66 with permission from Wiley, Copyright 2012.

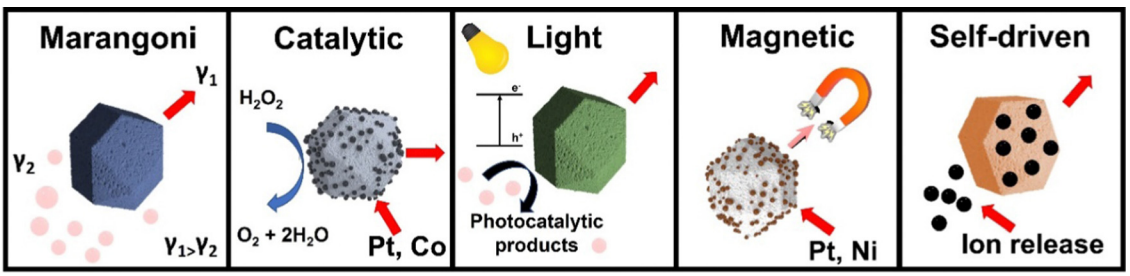

Fig. 2 Schematic of the main propulsion mechanisms of MOF MMs.

motion of the MMs by union and deactivation of the active sites, opening new avenues for motion-based sensing schemes.[59]

Apart from Janus-like morphologies, tubular catalytic MOF MMs have been synthesized, either by template electrodeposition or self-assembly routes. The aim yet is common, *i.e.*, to achieve dynamic processes exploiting and enhancing the unique properties of MOFs for adsorption, probe encapsulation, *etc.* Thus, kapok fibers were used as natural templates for the assembly of manganese dioxide as catalysts for peroxide decomposition and iron oxide nanoparticles. Subsequently, ZIF-8 MOFs were incorporated. After the removal of the template, the inner catalytic layer was exposed for catalytic action, whereas the ZIF-8 active sites were available for pollutants adsorption.[68] Herein the MOFs were 'passively' transported by a moving unit (a catalytic metal), but is a perfect example of the convenient combination of enhanced movement with MOFs to greatly accelerate common static processes. Similarly, iron doped ZIF-8/Pt microrods were prepared using a membrane as a template *via* filtration and electrochemical deposition. The resulting synergetic MMs display good features for dynamic uranium adsorption. While promising, the requirement of high levels of H_2O_2 raised concerns over biocompatibility for future applications.[69] As a response to such demands, biocatalytic MOFs containing catalytic enzymes as an alternative to metals were explored. The concept was illustrated by using catalase as a model enzyme and UiO-Zr MOFs. The MM benefits again from the unique properties of MOFs: high stability in water, mesoporous structure (from 6 to 10 nm size) for enzyme adsorption and an additional microporous network for product release-exchange-storage that can enhance the enzymatic reaction. Catalase was simply encapsulated by mixing it with the UiO-Zr MMs by adsorption, at an estimated rate of 0.21 ± 0.01 mg catalase per mg MOFs. The MMs show efficient propulsion at levels as low as 0.5% H_2O_2, opening new avenues for biocompatible MOF based MMs.[64] The concept can be extended with the use of other enzymes for propulsion in the

presence of the target substrate, which can be a (bio)-analyte. Challenges remain, yet, to achieve efficient motion in real-life settings, where the presence of co-existing proteins or the viscosity of the media can hamper or stop MM motions. So far, as will be described in the next section, these catalytic designs have been explored for proof-of-concept applications in the environmental and analytical realms, with some *in vitro* biomedical applications.

2.2 Current steps: cutting-edge developments in fuel-free propulsion

Fuel-free MOF MMs are currently a subject of intense study and current development in the field, with some recent interesting but few applications. As illustrated in Fig. 1, light driven, and magnetic propulsion designs have been explored. MIL based MOFs coated with a layer of the conductive polymer polypyrrole (PPy) were doped with methylene blue (MB) as a sensitizer molecule, resulting in a light responsive unit that can interact with VIS light. The MIL properties play a key role in the synthesis and further functionality. First, the limited solubility in water assures structural stability for the subsequent application. Secondly, the presence and subsequent release of Fe units from the MOFs allow for PPy polymerization for bonding of MB *via* π–π and electrostatic interactions. After irradiation with VIS light, electron and hole pairs are generated synergistically in the composite structure, which subsequently generate ionic products by reaction with the media for diffusiophoretic propulsion. Additionally, a thermal convection contribution in the motion mechanism is also introduced because of asymmetric irradiation of the liquid media. The radical oxygen species (ROS) generated during the MM motion were exploited for *in vitro* Hella cell disruption.[65] NIR light has been also explored for MOF-based MM propulsion. Thus, mesoporous polydopamine (PDA) nano bowls have been used both as a template and as a carrier of UiO-66 MOFs. The asymmetric PDA structure enhanced the interaction with NIR light, inducing a localized photothermal effect, which result in a gradient of temperature responsible for the thermophoretic MM propulsion. This is due to the excellent thermal conversion abilities of PDA. The enhanced surface properties of the UiO-66 are used here for MB adsorption in environmental applications.[70] On overall, MOFs in light driven MM designs act as passive components or templates for enhanced synthesis. More developments are expected soon exploiting the MOF properties as active units, especially the ability of these unique materials to incorporate light-sensitive units in the structure. Regarding the propulsion mechanism, while biocompatible, challenges remain, for example, potential interferences of other coexisting substances in the media with phoretic mechanisms or the low penetration ability of light in living tissues or water containing a high level of organic matter. Regarding magnetic propulsion, while magnetic units have been included in MOFs for direction control, few reports have been reported on magnetic driven MOFs, despite the high biocompatibility and advantages over light-driven mechanism, *i.e.*, the enhanced propulsion in viscous media and the ability for penetration into tissues. In this context, Pane's group synthesized magnetic helical microstructures as carriers/templates for ZIF-8 MOFs assembly. The carriers were helical structures, denoted as artificial bacterial flagella, prepared by laser writing, followed by modification with PDA. Next, the templates are used for the direct synthesis of the MOFs. The moving features of the MMs allow for targeted delivery to cancer cells, where the slightly acidic media can dissolve the ZIF-8 MOFs, which can be previously loaded with drugs.[66]

Additionally, the morphology and properties of MOFs have been explored to design alternative and cutting-edge fuel-free motion mechanisms where the actual MOFs is the moving unit without the requirements for additional microcarriers. Fig. 2 illustrates representative examples of these self-driven MOF MMs. Polyhedral shaped UiO-66, ZIF-8, MIL-88B, and MIL-96 MOFs have been propelled by the action of alternating current (AC) electric fields. The propulsion relies strongly on the polyhedral shape, which is broken by the action of the AC field, resulting in an unbalanced electrohydrodynamic flow, which propels the MMs at a speed of over 12 μm s^{-1} (1500 Hz).[71] In another interesting work, the (in some cases) degradation of MOFs in certain conditions has been used as a tool for the creation of gradients of ionic species and spontaneous ion diffusiophoretic propulsion. The self-fueled MMs were prepared by coating ZIF-90, ZIF-67, ZIF-8, MOF-5 and UiO-66 MOFs with an Au layer.[72] Yet, a main disadvantage of the phoretic propulsion mechanism is the interference due to the presence of electrolytes and viscosity in the media. While opening new avenues and modes of propulsion for MOF-based MMs, more developments are needed for the real-life application of this self-fueled propulsion in the near future, perhaps in combination with other propulsion modes or stimuli. Adaptive propulsion modes are also envisioned.

3. Expanding the applications of MOF micromotors

After describing the main propulsion mechanism, in this section, we will describe the applicability of MOF based MMs in diverse fields. Since previous reviews have covered the progress until 2021,[21,22,73,74] we will focus here on recent but vast applications, with special emphasis on non-catalytic schemes. For the reader's guidance, Table 1 shows a summary of MOF MM applications from 2018 to date.

3.1. Biomedical applications

The progress of MOF MMs in biomedical applications has followed a similar trend observed for propulsion mechanisms, with early proof-of-concept applications based on catalytic designs to fuel-free schemes. The main applications have been directed to drug delivery, due to the intrinsic MOFs properties (*i.e.*, large surface area) for drug encapsulation and the ability for dissolution in the tumour environment. Recent efforts have been aimed at the inactivation of malignant cells (cancer) and bacteria biofilms *via* drug encapsulation/delivery

Table 1 Applications of MOF based MMs

MOF	Propulsion	Ref.
Biomedical applications		
Drug delivery		
ZIF-67/Fe_3O_4	Catalytic (H_2O_2)	75
ZIF-L/catalase	Catalytic (H_2O_2) pH-responsive	76
ZIF-L/catalase	Catalytic (H_2O_2) pH-responsive	77
Polymeric helix-ZIF-8@Fe	Magnetic	78
CuS ZIF-8	NIR light	79
Cancer and bacteria cells destruction		
ZIF-8@Catalase/glucose oxidase	Catalytic (glucose/H_2O_2)	80
MIL/PPy/MB	VIS light	65
NH_2-MIL-101/glutathione hydrolase	Self-diffusiophoresis	81
ZIF-90-Au, ZIF-67-Au	Self-diffusiophoresis	72
Environmental remediation		
(Photo)-Fenton degradation of pollutants		
ZIF-Fe/PS/Ag	Catalytic (H_2O_2)	82
ZIF-8/ZnONPs@Fe_3O_4@AgNPs	Catalytic (H_2O_2)	83
ZIF-67/Fe_3O_4	Catalytic (H_2O_2)	84
Adsorptive removal of pollutants		
HRP-MIL-100(Fe)TiO_2@Fe_3O_4	Catalytic (H_2O_2)	85
Fe_3O_4-Fe-ZIF-8-Pt	Catalytic (H_2O_2)	69
ZIF-8/MnO_2/Fe_3O_4	Catalytic (H_2O_2)	68
ZIF-catalase	Catalytic (H_2O_2)	86
ZIF-67/Co	Catalytic (H_2O_2)	87
PDA@UiO-66	NIR light	70
$MnFe_2O_4$@MIL-53@UiO-66 @MnO_2	Magnetic catalytic (H_2O_2)	88
Fe_3O_4@NH_2-UiO-66/Pt	Catalytic (H_2O_2)	89
Analytical sensing		
CuJAST-1/diphenylalanine peptide	Chemotaxis	63
Eu-MOF/EDTA-NiAl-CLDH/MnO_2	Catalytic (H_2O_2)	90
PCL/COF/MnO_2	Catalytic (H_2O_2)	91
ZIF-8/Catalase/glucose oxidase	Catalytic (glucose)	92

or sophisticated mechanisms by the production of ROS during the self-propulsion of the MMs (see Table 1 for more details).

One of the first designs for drug delivery compromised ZIF-67 units, with unique mesoporous and microporous structures for the encapsulation of doxorubicin (DOX). The MMs propel by catalytic decomposition of H_2O_2 in the Co catalytic sites, while Fe_3O_4 nanoparticles were self-assembled in the structure for controlled magnetic guidance. The fuel induced the drug release from the ZIF-67 by conformational changes and promoted its dissolution, enhancing the release.[75] Due to the use of the toxic fuel, *in vitro* or *in vivo* applications were not described. For enhanced biocompatibility, two biocatalytic designs using ZIF-L as a carrier for the encapsulation of catalase as a catalyst were described. The large pores allow the assembly of catalase for peroxide decomposition, whereas the inclusion of succinylated β-lactoglobulin (β-LG)[76] or poly(2-diisopropylamino)ethyl methacrylate polymer (PDPA)[77] allows ON–OFF speed regulation and buoyancy motion control by pH changes. In the case β-LG modified MMs, such protein is permeable at neutral pH, allowing the access of H_2O_2 to the catalase encapsulated in the ZIF-L for efficient motion. At acidic pH, β-LG gelation hampers the access of the fuel, resulting in a hampered motion. Next, the MMs were loaded with DOX and used for its delivery to HeLa cancer cells. The acidic tumour microenvironment accelerates the MM speed for enhanced delivery, although further *in vivo* studies are required to assess the overall biocompatibility of the MMs.[76] In the case of PDPA modified MMs, at pH higher than 6.4 the amine groups in PDPA are deprotonated, increasing the hydrophobicity. As such, the oxygen bubbles produced by the catalytic reaction of peroxide with catalase bind to the PDPA, increasing the buoyancy of the particles, which experience an ascending motion. At pH lower than 6.4, the amine groups in PDPA are protonated and the polymer is hydrophilic. Thus, the oxygen gas bubbles are expelled and the micromotors experience a descending motion.[77] As a proof-of-the-concept, fluorouracil loaded MMs were used as moving carriers in a three-dimensional cell culture device with MCF-7 cells at pH 6.3 and 7.4. In both cases, efficient cancer cell destruction was observed, which indicates that the MMs were successfully internalized in the cells.[77] These relevant examples of biocatalytic MMs benefits from the combination with MOFs for the introduction of a higher loading of enzyme catalysts-due to the unique structure and high surface area of MOFs-along with the unique geometrical features with play a key role in to design stimulate responsive drug delivery systems, propelled at non-toxic H_2O_2 levels. In a most sophisticated study, ZIF-8 MOFs were functionalized with upconversion nanoparticles (UCNPs) and the enzymatic pair catalase/glucose oxidase. The latter enzyme oxidises intracellular glucose leading to its decomposition, which causes starvation of the cells and generates ROS, between stand out H_2O_2, which is used as fuel for catalase and

MM catalytic motion. The UCNPS interact with NIR light for photodynamic therapy for highly efficient cancer cell inactivation.[80] More studies are needed, yet, to evaluate the *in vivo* performance of these systems and complex media that can deactivate the enzyme catalyst or hamper the MM motion.

Biocatalytic MOF MMs opened a new avenue in novel drug delivery application designs. To circumvent some of the above-mentioned disadvantages (*i.e.*, avoid the use of peroxide fuel, even at non-toxic levels, prolonged motion, *etc.*) other external sources of propulsion such as NIR light and magnetic fields were explored. In the first example, as shown in Fig. 3A(a), Pane's group tailored the previously reported concept of MOFs magnetic MMs,[66] towards fully biocompatible and biodegradable drug delivery systems. As such, ZIF-8@Fe MOFs loaded with DOX were assembled in gelatin methacryloyl helices prepared by laser writing. The magnetic particles introduced in the MOFs allow for efficient magnetic propulsion, with motion enhanced by the helical shape of the carriers (see the motion patterns in Fig. 3A(b)). The MM is fully biodegradable, by enzymes and by acidic pH (the MOF part). Successful DOX delivery into Hella cells is illustrated in Fig. 3A(c), revealing further cell inactivation and death.[78] NIR light can be also a convenient stimulant for MMs propulsion due to its biocompatibility. CuS nanoparticles coated with ZIF-8 MOFs display efficient motion after NIR light irradiation, exploiting the heat absorbing properties of Cu and the bowl-shape of the MMs. This allows targeted delivery and penetration into cancer cells. *in vitro* studies conducted in MCF-7 cells illustrated the multifunctional capabilities of the MMs, which combined enhanced ROS generation by Cu along pH degradation of ZIF, which can be used for encapsulation of drugs (see Fig. 3B(a)). *In vivo* studies further confirm the feasibility of the MM based strategy, with reduced tumour size when using the MMs as compared with control experiments or static conditions.[79]

Additional mechanisms for cancer and cell deactivation using MOF MMs exploit potential ROS generation or interferences with metabolites and signalling elements for inactivation, avoiding the use of DOX or additional drugs and additional co-reagents. Pumera's group employed VIS light driven MIL/PPy/MB (for the propulsion mechanism, see the previous section) for cervix carcinoma HeLa cell destruction. The mechanism relies on the MM accumulation in the tumour area (induced by its collective behaviour) along with a combination of ROS generation and photothermal action due to the

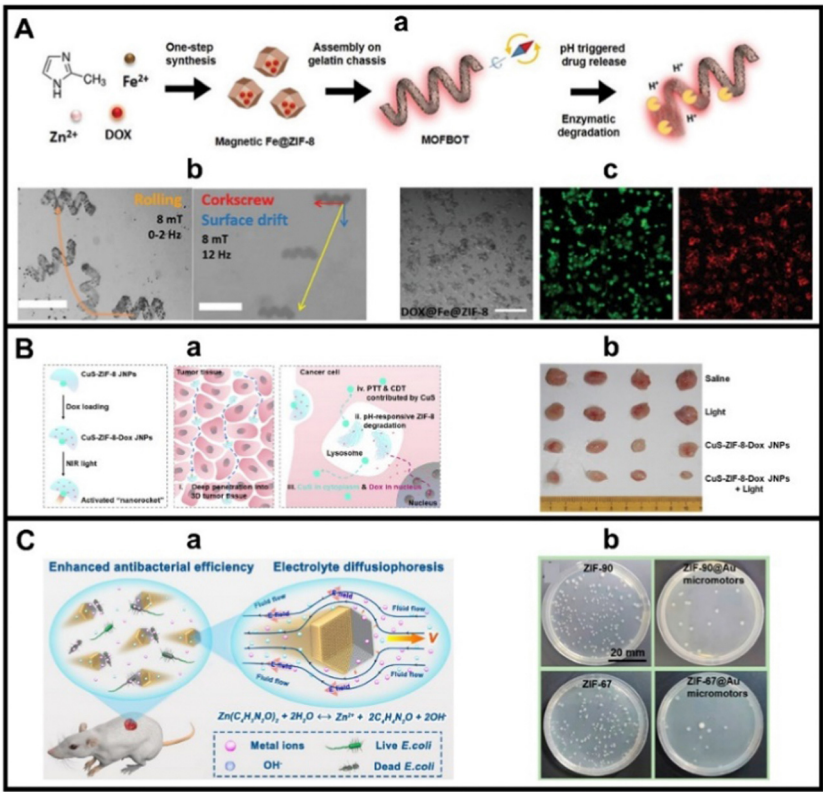

Fig. 3 MOF MMs for biomedical applications. (A) Magnetic propelled ZIF-8@Fe MMs for DOX delivery: (a) schematic of the synthesis procedure and drug release; (b) time-lapse microscopy images of the magnetic propulsion into rolling and corkscrew patterns and (c) images of HeLa cells and LIVE/DEAD staining images (in green and red, respectively) after incubation with the MMs, where all cells are dead as indicated by the intense red staining. (B) CuS-ZIF-8 NIR propelled MMs for drug delivery: (a) schematic of the synthesis/propulsion and cancer cell penetration mechanism and (b) images of dissected tumours corresponding to *in vivo* studies performed in rat models. (C) Self-fueled MMs for bacteria biofilm inactivation: (a) schematic of the propulsion mechanism and bacteria inactivation *via* ROS generation and (b) pictures of bacteria colonies in the presence of not moving and moving MMs. Reproduced from ref. 78 with permission from Wiley, copyright 2020 (A); ref. 79 with permission from Elsevier, copyright 2002 (B) and ref. 72 with permissions from American Chemical Society, copyright 2022 (C).

photophoretic mechanism.[65] In another excellent example of cooperative MOFs MM action, NH_2-MIL-101 based MMs were assembled by asymmetric modification with polyethylene glycol and glutathione hydrolase γ-glutamyltransferase. The MMs exhibit a chemotactic effect induced by the excess of glutathione in tumours. This induces its accumulation in cancer areas. As the MOFs are loaded with Erastin, a ferroptosis inducer, interfere with the metabolism of the malignant cells and induce an excess of Fe^{2+}, generating ROS through the Fenton reaction, leading to the death of tumour cells.[81] Self-fuelled ZIF-90 and ZIF-67 MMs (for details in the propulsion mechanism, see the previous section) during its motion and self-destruction release Zn and Co ions that were effective to deactivate *Escherichia coli* bacteria by electrostatic interaction and disruption of the cell membrane (see Fig. 3C). As can be seen, biomedical applications of MOF MMs are vast and have evolved from catalytic designs to synergetic models combining catalytic with NIR light activation or cooperative action, exploiting the joining effect of swarms of MMs with chemicals released during its motion for highly efficient and non-toxic cancer and other cells inactivation systems.[72]

3.2. Environmental remediation

Environmental applications using MOF MMs explored the inherent advantages of the materials, such as the high surface area, for pollutant adsorption and the tailorability to include catalytic metals for Fenton-based degradation processes. One of the first MOF MMs for water decontamination was designed by coating polystyrene nanoparticles with a half-layer of Ag for propulsion using H_2O_2 and a half-layer coated with ZIF-Zn–Fe MOFs. The Ag layer plays a key role in the degradation, with the combination of adsorption and OH generation *via* Fe sites. Rhodamine B (RhB, 20 mg L^{-1}) was used as a model dye, achieving 94% degradation after 150 minutes of treatment using 12% H_2O_2.[82] In this early design, the MOFs act as a "passive" units assembled in a moving unit, as already observed in early biomedical applications. Yet, the high concentration of peroxide used prevents the application in real life settings. Composite based MOF MMs were later synthesized using microdroplets as templates. The synthesis is performed with the aid of microfluidics, for spatial assembly of Fe_3O_4@Ag nanoparticles on one size ZIF-8@ZnO nanoparticles at the other. Such different parts results in a synergetic MM for RhB degradation, *i.e.*, the iron and Ag containing part act as the propulsion units, generating oxygen bubbles after reaction with H_2O_2, while the MOF size allows for enrichment of the pollutant and OH radical generation (after irradiation with UV light), resulting in a degradation efficiency close to 100% in 60 min.[83] ZIF-67/Fe_3O_4 MMs have been also exploited recently for Fenton degradation, using the cobalt core and iron ions as active centres for OH generation and peroxide decomposition for efficient propulsion.[84] Still, in these two strategies, relatively high concentrations of peroxide fuel are used.

Another set of strategies using MOF MMs in the environmental realm explored the exceptional surface properties and mesoporous structure for pollutants adsorption. Heavy metals and organic pollutants have been the main targets. Pumera's group employed template prepared iron doped Fe_3O_4/ZIF-8/Pt microrods for uranium removal. Excellent removal efficiencies of up to 96% are obtained after 1 h motion in 1% peroxide solutions, with only 13% removal using the static MMs under magnetic agitation. The removal efficiency was attributed mainly to the adsorption of uranium by the MOFs.[69] While efficient, Pt is a catalyst with a high overall associated cost, which can hamper the application for full scale treatment that requires the use of higher amounts of MMs. As an alternative, $MnFe_2O_4$ was used as a template for the assembly of MIL-53 MOFs, which was then covered with UiO-66 MOFs. Finally, MnO_2 nanoparticles were assembled for catalytic propulsion, as an alternative catalyst of Pt. The presence of –COOH groups in the UiO-66, along with the enhanced stability, allows for the removal of Pb and Cd from contaminated water *via* chelation, with 80% removal efficiencies and reusability over repetitive cycles of treatment, greatly reducing the costs for potential full-scale applications.[88] Tubular designs relying on MnO_2 as a catalyst have been prepared by assembling ZIF-8 in γ-Fe_2O_3/γ-Al_2O_3/MnO_2 microtubes for Congo red and doxycycline adsorptive removal.[68] As an alternative to metal catalysts, the versatility of the previously described catalase based MMs[76,77] allow for its application in the removal of heavy metals and perfluorooctanoic acid, a highly persistent pollutant. The catalase-encapsulation MMs experience a buoyancy effect motion in the presence of peroxide fuel, for adsorptive removal of the pollutants.[86] Recent trends in the last year have been aimed at the design of fuel-free and more efficient MOF based MMs for realistic application in the environmental realms. The strategies developed so far in this context are depicted in Fig. 4. More efforts are envisioned soon.

Fig. 4. Illustrates the use of Fe_3O_4@NH_2-UiO-66 MOF MMs for the adsorptive removal of pollutants, combining the efficient MM motion with the remarkably high surface area of MOFs. MMs are prepared on a mass scale by Pickering emulsion assembly for future scalability. While still Pt is used for propulsion, it can be easily replaced by other catalysts or active units to achieve other fuel-free propulsion modes. The large-scale assembly is achieved by mixing Fe-UiO nanoparticles suspended in water with an *n*-butanol solution using a high-speed stirrer. This induces the spontaneous adsorption of the Fe-UiO nanoparticles at the water/organic solution and the as-generated drops gradually shrink, ultimately leading to the MM hollow structure. The MMs can propel in 5% H_2O_2 solution for the efficient adsorptive removal of methyl orange and Cr (with removal percentages higher than 90%) in 60 min.[89] As an alternative to peroxide propulsion, bowl-shaped UiO-66 MOF MMs modified with PDA were reported. The asymmetric shape and the thermal conversion abilities of the PDA results in the efficient MM propulsion by irradiation with NIR light (see Fig. 4B), with the "passive" moving MOFs acting as highly efficient platforms for the adsorptive removal of MB. The mechanism of removal is mainly attributed to π–π interaction of the aromatic rings of MB with the UiO active groups. Here the MOFs play a key role in the enhanced removal attributed to

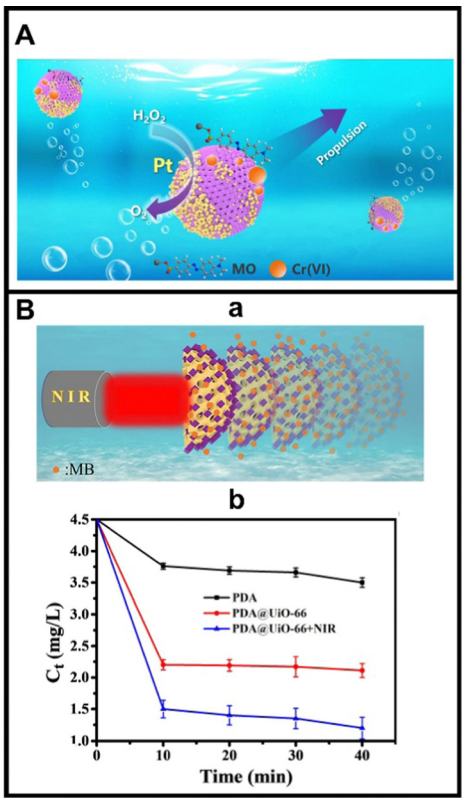

Fig. 4 MOF MMs for environmental remediation applications. (A) Fe_3O_4@NH_2-UiO-66 MOF based colloidosome MMs for the adsorptive removal of dyes and heavy metals. (B) NIR propelled PDA@UiO-66 MMs for dye removal: (a) schematic of the propulsion, (b) plot showing the variation of the concentration over time of the MB after treatment with PDA, static and moving MMs. Reproduced from ref. 89 with permission from Wiley, copyright 2022 (A) and ref. 70 with permission from Elsevier, copyright 2022 (B).

their high specific surface area and porous structure, as illustrated in Fig. 4A(b).[70] Indeed, higher removal efficiencies are obtained when using the moving MM, as compared with PDA and static counterparts. Cutting-edge trends in the field are aimed at the simultaneous removal and detection of pollutants by exploiting the mesoporous structure of more and the wide available sites for enzyme encapsulation. MIL-100(Fe)@TiO_2@-Fe_3O_4 Janus MMs have been modified with horseradish peroxidase (HRP) for simultaneous removal and detection of hydroquinone. The multifunctional structure contains Mn_2O_3 as a catalyst for the decomposition of H_2O_2 for efficient propulsion, while HRP and the MIL MOF part promote –OH and $-O^{2-}$ radicals' generation. Colorimetric detection was achieved in connection with 3,3′,5,5′-tetramethylbenzidine (TMB). An increase in the concentration of hydroquinone inhibits the TMB conversion to its blue coloured product, resulting in an increase in the absorbance of the solution that can be related to hydroquinone concentration, with a linear range of 2–240 μm. Hydroquinone removal was achieved by sunlight induced Fenton degradation exploiting the radical generation and the MIL-100(Fe)@TiO_2 heterojunction.[85] The latter work opens new opportunities towards fuel-free or light driven MOFs for environmentally friendly pollutant removal. This field still needs more exploration, with relatively few developments if compared with the progress of MOF MMs with biomedical applications, where even *in vivo* studies are available.

3.3. Analytical sensing

MMs are extremely convenient for analytical sensing applications, particularly bubble-propelled designs. Indeed, the enhanced fluid mixing accelerated convection of the MMs greatly decreases the detection time and allows to use of μL volumes of samples, which is of special interest in the analysis of hard to obtain clinical samples (neonates blood, cerebrospinal fluid, *etc.*) or forensics samples such as vitreous humour.[31,93] MOFs themselves are also considerably attractive for analytical applications, ranging from their use as sorbents in sample preparation, as stationary phases in chromatographic separation columns or as substrates for enzyme and probes immobilization in biosensors.[94,95] Despite this promising combination, scarce approaches of MOF based MMs in analytical sensing have been reported to date. Early developments in this direction were reported in 2015 with the above-described Marangoni based MOF MMs for heavy metal sensing. Since then, only 3 articles have been published describing the use of MOF MMs for fluorescence and electrochemical sensing.[63] Two representative examples are depicted in Fig. 5. Fluorescence sensing of Fe has been achieved by using Eu doped outer MOF layer with an inner catalytic MnO_2 layer (see Fig. 5A(a) for the MMs structure and mechanism). The MMs are synthesized using kapot fibre as templates. The enhanced MMs movement in the presence of H_2O_2 results in a highly efficient platform for OFF–ON detection of Fe based on the adsorption on the MOF-Eu layer, producing a quenching in the native fluorescence by competitive adsorption and electron transfer see Fig. 5A(b). A limit of detection of 0.15 μM was achieved, with high selectivity.[90] Covalent organic frameworks have been also encapsulated in polycaprolactone/MnO_2 catalytic MMs for OFF–ON fluorescence detection of nitroaromatic explosives.[91] In a very sophisticated recent approach, biocatalytic ZIF-8 MMs encapsulating the pair glucose oxidase/catalase have been used to develop a new concept of vertical collision and electrochemical detection (see Fig. 5B). In the presence of glucose in the electrochemical cell, enzyme cascade reactions are initiated, generating peroxide from glucose enzymatic decomposition, which as a substrate for catalase, initiating the motion. Due to the buoyancy effect, the MMs collapse with the electrodes, generating spike signals. The number of signal spikes increases with the increase in glucose concentration, holding considerable promise for its determination.[92] All these representative MOFs-MM based approaches represent their potential for novel analytical applications, which are expected to be developed soon.

4. Challenges in the future development of MOF micromotors

This article highlights recent trends in the design and application of MOF based MMs. We have identified that the combination of

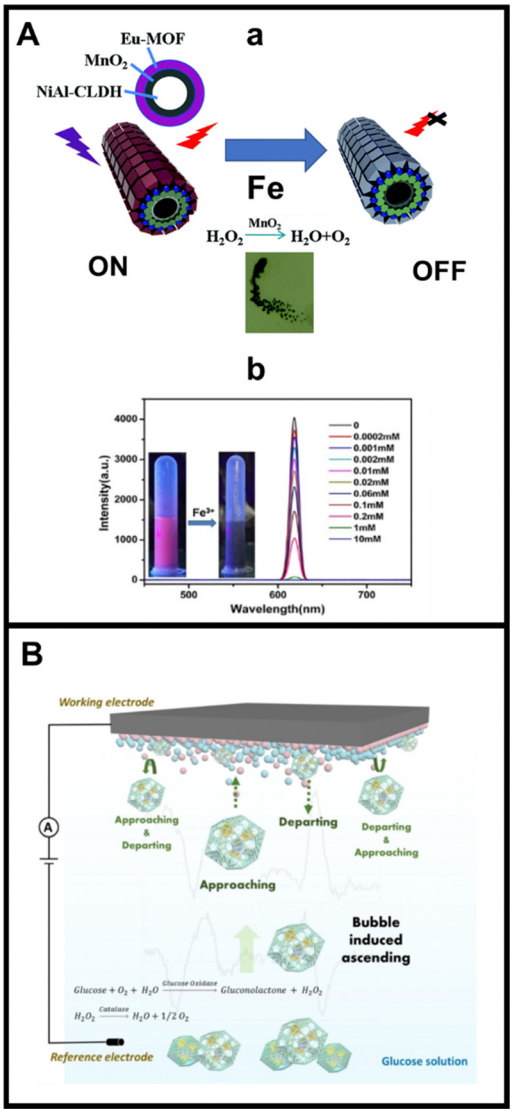

Fig. 5 MOF MMs for analytical sensing. (A) (a) Eu based MOF MMs for ON–OFF fluorescence sensing of Fe ions; (b) schematic of the detection and fluorescence spectra of the quenching of MMs at increasing concentrations of Fe with photographs taken under UV light showing the original and the quenched fluorescence upon addition of Fe ions. (B) Biocatalytic ZIF-8/glucose oxidase/catalase MMs for electrochemical collision mechanism for glucose detection. Reproduced from ref. 90 with permission from the Royal Society of Chemistry, copyright 2019 (A) and ref. 92 with permission from Wiley, copyright 2022 (B).

the excellent properties of MOFs (micro and mesoporous structure, easy synthesis, presence of functional groups for modifications, among others) with the moving properties of MMs have led to a new generation of moving nanovehicles with high potential for many relevant applications in diverse fields.

Material aspects play a key role in the design of MOF MMs, as stability in water and biocompatibility must be considered. From early works in the field in 2015 on Marangoni-propelled designs, the field has evolved into more sophisticated and adaptative mechanisms. Many designs have been proposed, from using MOFs as passive units and a propulsion chassis as carriers to sophisticated moving MOFs incorporating catalytic units or optimal shapes for manipulation with external energies. For the design of catalytic-propelled MMs, driven by peroxide fuels, UiO MOFs were preferred over ZIF due to their stability. Both Co and Pt have been used as catalysts, later replaced by catalase enzyme towards increased biocompatibility and motion at ultralow peroxide levels. Recent sophisticated motion mechanisms explore the instability of MOFs (such as ZIF types) as self-fuelled units for efficient self-electrophoretic propulsion and release of radicals for sophisticated operations. Challenges remain on the interferences of a constituent in the media on the motion. As an alternative, AC fields or the use of magnetic carriers and light-driven propulsion hold considerable promise for prolonged motion in real settings. An additional advantage is the ability of these designs to act cooperatively as a swarm, really enhancing the efficiency of the intended application.

We have also highlighted the direction of MOF MMs in diverse fields. Vast progress has been achieved in the biomedical field, especially with the recent blooming of fuel-free MOF designs. Main aims have been targeted drug delivery and cancer cell destruction applications. In this sense, ZIF-based MOFs possess several advantages for drug encapsulation and disintegration at the native acidic pH in cancer cells, with magnetic carriers or VIS light propulsion acting as the driving force to reach the targeted tissue. *In vitro* applications have led to preliminary but promising *in vivo* applications in rat models. Challenges remain in further biocompatibility studies and MMs tracking/recovery or degradation in the human body. Compared with the vast progress in the biomedical field, environmental applications of MOFs still rely strongly on peroxide propulsion, with only one example of a NIR propelled design. While peroxide is desirable in the Fenton process, its use should be avoided in high quantities, as it can represent a toxic itself. Another issue, common to MMs application for pollutant treatment, is the large-scale production and application of MMs for the treatment of high-water quantities. In this context, recent studies on Pickering emulsion-prepared MOF MMs, using low-cost catalysts in connection with the excellent sorption/catalytic properties of MOFs, could help to solve the above-mentioned need. Regarding the analytical field, scarce but promising fluorescence and electrochemical detection applications have been reported. New directions might be aimed to explore the potential of such procedures in the analysis of complex clinical samples, available in few quantities, in the field of diagnosis, due to the low sample volumes required and the fast detection times.

Overall, even though, as expected, the main application of MMs based on MOFs has been identified in the biomedical field, we envision a development soon in the environmental and biosensing fields. Using creatively the possibilities of molecular recognition in connection with the structural and surface properties of MOFs, an improvement in the efficiency of clean up on the fly procedures and preconcentration processes and more effective biosensing on suitable functionalized and decorated MOF surfaces, is highly expected.

Author contributions

Javier Bujalance-Fernández: conceptualization, writing – original draft Writing – review & editing. Beatriz Jurado-Sánchez: conceptualization, funding acquisition, project administration, resources, supervision, writing – original draft, writing – review & editing. Alberto Escarpa: conceptualization, funding acquisition, project administration, resources, supervision, writing – review & editing.

Abbreviations

AC	Alternating current
BDC	1,4-Benzenedicarboxylate
β-LG	β-Lactoglobulin
DOX	Doxorubicin
DPA	Diphenylalanine
HRP	Horseradish peroxidase
MB	Methylene blue
MeIM	Imidazole
MIL	Materials institute lavoisier
MMs	Micromotors
MOFs	Metal–organic frameworks
PDA	Polydopamine
PDPA	Poly(2-diisopropylamino)ethyl methacrylate polymer
PPy	Polypyrrole
RhB	Rhodamine B
ROS	Radical oxygen species
TMB	3,3′,5,5′-Tetramethylbenzidine
UCNPs	Up conversion nanoparticles
UiO	University of Oslo
ZIF	Zeolitic imidazolate frameworks.

Conflicts of interest

There are no conflicts to declare.

Acknowledgements

This work was supported by Grant PID2020-118154GB-I00 funded by MCIN/AEI/10.13039/501100011033 (A. E and B. J. S); grant TED2021-132720B-I00, funded by MCIN/AEI/10.13039/501100011033 and the European Union "NextGenerationEU"/PRTR (A. E and B. J. S); the Community of Madrid [grant numbers CM/JIN/2021-012 (B. J. S), TRANSNANOAVANSENS, S2018/NMT-4349 (A. E)] and the Universidad de Alcalá [FPI contract, Plan Propio UAH (J. B. F)].

References

1 Y. Li, G. Wen, J. Li, Q. Li, H. Zhang, B. Tao and J. Zhang, *Chem. Commun.*, 2022, **58**, 11488–11506.
2 H. Zhou, J. R. Long and O. M. Yaghi, *Chem. Rev.*, 2012, **112**, 673–674.
3 H.-C. J. Zhou and S. Kitagawa, *Chem. Soc. Rev.*, 2014, **43**, 5415–5418.
4 V. F. Yusuf, N. I. Malek and S. K. Kailasa, *ACS Omega*, 2022, **7**, 44507–44531.
5 P. Deria, J. E. Mondloch, O. Karagiaridi, W. Bury, J. T. Hupp and O. K. Farha, *Chem. Soc. Rev.*, 2014, **43**, 5896–5912.
6 A. J. Howarth, Y. Liu, P. Li, Z. Li, T. C. Wang, J. T. Hupp and O. K. Farha, *Nat. Rev. Mater.*, 2016, **1**, 15018.
7 S. L. Griffin and N. R. Champness, *Coord. Chem. Rev.*, 2020, **414**, 213295.
8 P. Iacomi and G. Maurin, *ACS Appl. Mater. Interfaces*, 2021, **13**, 50602–50642.
9 K. Noh, J. Lee and J. Kim, *Isr. J. Chem.*, 2018, **58**, 1075–1088.
10 S. Yang, X. Li, G. Zeng, M. Cheng, D. Huang, Y. Liu, C. Zhou, W. Xiong, Y. Yang, W. Wang and G. Zhang, *Coord. Chem. Rev.*, 2021, **438**, 213874.
11 L. Valenzano, B. Civalleri, S. Chavan, S. Bordiga, M. H. Nilsen, S. Jakobsen, K. P. Lillerud and C. Lamberti, *Chem. Mater.*, 2011, **23**, 1700–1718.
12 S. Ma and H.-C. Zhou, *Chem. Commun.*, 2010, **46**, 44–53.
13 W. Zhou, Y. Tang, X. Zhang, S. Zhang, H. Xue and H. Pang, *Coord. Chem. Rev.*, 2023, **477**, 214949.
14 D. Ragab, H. G. Gomaa, R. Sabouni, M. Salem, M. Ren and J. Zhu, *Chem. Eng. J.*, 2016, **300**, 273–279.
15 M. Safaei, M. M. Foroughi, N. Ebrahimpoor, S. Jahani, A. Omidi and M. Khatami, *Trends Anal. Chem.*, 2019, **118**, 401–425.
16 Z. Hu, B. J. Deibert and J. Li, *Chem. Soc. Rev.*, 2014, **43**, 5815–5840.
17 Z. Sun, T. Li, T. Mei, Y. Liu, K. Wu, W. Le and Y. Hu, *J. Mater. Chem. B*, 2023, **11**, 3273–3294.
18 L. Jiao, J. Y. R. Seow, W. S. Skinner, Z. U. Wang and H.-L. Jiang, *Mater. Today*, 2019, **27**, 43–68.
19 Y.-S. Ho and H.-Z. Fu, *Inorg. Chem. Commun.*, 2016, **73**, 174–182.
20 C. W. Jones, *JACS Au*, 2022, **2**, 1504–1505.
21 A. Terzopoulou, J. D. Nicholas, X.-Z. Chen, B. J. Nelson, S. Pané and J. Puigmartí-Luis, *Chem. Rev.*, 2020, **120**, 11175–11193.
22 B. Khezri and M. Pumera, *Adv. Mater.*, 2019, **31**, 1806530.
23 A. S. Varela, W. Ju and P. Strasser, *Adv. Energy Mater.*, 2018, **8**, 1703614.
24 A. J. Howarth, A. W. Peters, N. A. Vermeulen, T. C. Wang, J. T. Hupp and O. K. Farha, *Chem. Mater.*, 2017, **29**, 26–39.
25 G. A. Ozin, I. Manners, S. Fournier-Bidoz and A. Arsenault, *Adv. Mater.*, 2005, **17**, 3011–3018.
26 J. Wang, *Nanomachines: Fundamentals and Applications*, Wiley, 2013.
27 W. F. Paxton, K. C. Kistler, C. C. Olmeda, A. Sen, S. K. Angelo, Y. Cao, T. E. Mallouk, P. E. Lammert and V. H. Crespi, *J. Am. Chem. Soc.*, 2004, **126**, 13424–13431.
28 L. Cai, D. Xu, Z. Zhang, N. Li and Y. Zhao, *Research*, 2023, **6**, 0044.
29 F. Zhang, J. Zhuang, Z. Li, H. Gong, B. Estaban-Fernández de Ávila, Y. Duan, Q. Zhang, J. Zhou, L. Yin, E. Karshalev, W. Gao, V. Nizet, R. H. Fang, L. Zhang and J. Wang, *Nat. Mater.*, 2022, **21**, 1324–1332.
30 P. Wrede, O. Degtyaruk, S. K. Kalva, X. L. Deán-Ben, U. Bozuyuk, A. Aghakhani, B. Akolpoglu, M. Sitti and D. Razansky, *Sci. Adv.*, 2022, **8**, eabm9132.
31 J. Wang, *Biosens. Bioelectron.*, 2016, **76**, 234–242.
32 E. Karshalev, B. Esteban-Fernández de Ávila and J. Wang, *J. Am. Chem. Soc.*, 2018, **140**, 3810–3820.
33 W. Gao, S. Sattayasamitsathit, J. Orozco and J. Wang, *J. Am. Chem. Soc.*, 2011, **133**, 11862–11864.
34 R. Maria-Hormigos, B. Jurado-Sanchez, L. Vazquez and A. Escarpa, *Chem. Mater.*, 2016, **28**, 8962–8970.
35 Y. Mei, A. A. Solovev, S. Sanchez and O. G. Schmidt, *Chem. Soc. Rev.*, 2011, **40**, 2109–2119.
36 L. Baptista-Pires, J. Orozco, P. Guardia and A. Merkoçi, *Small*, 2018, **14**, 1702746.
37 W. Gao, M. Liu, L. Liu, H. Zhang, B. Dong and C. Y. Li, *Nanoscale*, 2015, **7**, 13918–13923.
38 B. Jurado-Sánchez, M. Pacheco, J. Rojo and A. Escarpa, *Angew. Chem., Int. Ed.*, 2017, **56**, 6957–6961.
39 V. de la Asunción-Nadal, B. Jurado-Sánchez, L. Vázquez and A. Escarpa, *Chem. – Eur. J.*, 2019, **25**, 13157–13163.
40 W. Wang, W. Duan, S. Ahmed, T. E. Mallouk and A. Sen, *Nano Tod.*, 2013, **8**, 531–554.
41 W. Wang, L. A. Castro, M. Hoyos and T. E. Mallouk, *ACS Nano*, 2012, **6**, 6122–6132.
42 V. Garcia-Gradilla, J. Orozco, S. Sattayasamitsathit, F. Soto, F. Kuralay, A. Pourazary, A. Katzenberg, W. Gao, Y. Shen and J. Wang, *ACS Nano*, 2013, **7**, 9232–9240.
43 Z. Wu, T. Li, J. Li, W. Gao, T. Xu, C. Christianson, W. Gao, M. Galarnyk, Q. He, L. Zhang and J. Wang, *ACS Nano*, 2014, **8**, 12041–12048.

44 Y. Dong, L. Wang, V. Iacovacci, X. Wang, L. Zhang and B. J. Nelson, *Matter*, 2022, **5**, 77–109.
45 M. A. Zeeshan, R. Grisch, E. Pellicer, K. M. Sivaraman, K. E. Peyer, J. Sort, B. Özkale, M. S. Sakar, B. J. Nelson and S. Pané, *Small*, 2014, **10**, 1284–1288.
46 J. Wang, Z. Xiong, J. Zheng, X. Zhan and J. Tang, *Acc. Chem. Res.*, 2018, **51**, 1957–1965.
47 L. Xu, F. Mou, H. Gong, M. Luo and J. Guan, *Chem. Soc. Rev.*, 2017, **46**, 6905–6926.
48 Y. Mu, W. Duan, K. Y. Hsu, Z. Wang, W. Xu and Y. Wang, *ACS Appl. Mater. Interfaces*, 2022, **14**, 57113–57121.
49 Z. Wang, Y. Mu, D. Lyu, M. Wu, J. Li, Z. Wang and Y. Wang, *Curr. Opin. Colloid Interface Sci.*, 2022, **61**, 101608.
50 M. Sindoro, A.-Y. Jee and S. Granick, *Chem. Commun.*, 2013, **49**, 9576–9578.
51 H. Ahmed, X. Yang, Y. Ehrnst, N. N. Jeorje, S. Marqus, P. C. Sherrell, A. El Ghazaly, J. Rosen, A. R. Rezk and L. Y. Yeo, *Nanoscale Horiz.*, 2020, **5**, 1050–1057.
52 W. Gao, S. Sattayasamitsathit, A. Uygun, A. Pei, A. Ponedal and J. Wang, *Nanoscale*, 2012, **4**, 2447–2453.
53 A. Martín, B. Jurado-Sánchez, A. Escarpa and J. Wang, *Small*, 2015, **11**, 3568–3574.
54 V. V. Singh, K. Kaufmann, B. E.-F. de Ávila, E. Karshalev and J. Wang, *Adv. Funct. Mater.*, 2016, **26**, 6270–6278.
55 V. de la Asunción-Nadal, C. Franco, A. Veciana, S. Ning, A. Terzopoulou, S. Sevim, X.-Z. Chen, D. Gong, J. Cai, P. D. Wendel-Garcia, B. Jurado-Sánchez, A. Escarpa, J. Puigmartí-Luis and S. Pané, *Small*, 2022, **18**, 2203821.
56 C. C. Mayorga-Martinez, J. Vyskočil, F. Novotný and M. Pumera, *J. Mater. Chem. A*, 2021, **9**, 14904–14910.
57 Y. Ikezoe, G. Washino, T. Uemura, S. Kitagawa and H. Matsui, *Nat. Mater.*, 2012, **11**, 1081–1085.
58 T. T. Y. Tan, J. T. M. Cham, M. R. Reithofer, T. S. Andy Hor and J. M. Chin, *Chem. Commun.*, 2014, **50**, 15175–15178.
59 J. Li, X. Yu, M. Xu, W. Liu, E. Sandraz, H. Lan, J. Wang and S. M. Cohen, *J. Am. Chem. Soc.*, 2017, **139**, 611–614.
60 T. H. Seah, G. Zhao and M. Pumera, *ChemPlusChem*, 2013, **78**, 395–397.
61 G. Zhao and M. Pumera, *Lab Chip*, 2014, **14**, 2818–2823.
62 J. Orozco, D. Vilela, G. Valdés-Ramírez, Y. Fedorak, A. Escarpa, R. Vazquez-Duhalt and J. Wang, *Chem. – Eur. J.*, 2014, **20**, 2866–2871.
63 Y. Ikezoe, J. Fang, T. L. Wasik, M. Shi, T. Uemura, S. Kitagawa and H. Matsui, *Nano Lett.*, 2015, **15**, 4019–4023.
64 Y. Yang, X. Arqué, T. Patiño, V. Guillerm, P.-R. Blersch, J. Pérez-Carvajal, I. Imaz, D. Maspoch and S. Sánchez, *J. Am. Chem. Soc.*, 2020, **142**, 20962–20967.
65 L. Dekanovsky, Y. Ying, J. Zelenka, J. Plutnar, S. M. Beladi-Mousavi, I. Křížová, F. Novotný, T. Ruml and M. Pumera, *Adv. Funct. Mater.*, 2022, **32**, 2205062.
66 X. Wang, X.-Z. Chen, C. C. J. Alcântara, S. Sevim, M. Hoop, A. Terzopoulou, C. de Marco, C. Hu, A. J. de Mello, P. Falcaro, S. Furukawa, B. J. Nelson, J. Puigmartí-Luis and S. Pané, *Adv. Mater.*, 2019, **31**, 1901592.
67 A. Ayala, C. Carbonell, I. Imaz and D. Maspoch, *Chem. Commun.*, 2016, **52**, 5096–5099.
68 J. Liu, J. Li, G. Wang, W. Yang, J. Yang and Y. Liu, *J. Colloid Interface Sci.*, 2019, **555**, 234–244.
69 Y. Ying, A. M. Pourrahimi, Z. Sofer, S. Matějková and M. Pumera, *ACS Nano*, 2019, **13**, 11477–11487.
70 Y. Zhao, D. Wang, Y. Luan and X. Du, *Mater. Today Sustain.*, 2022, **18**, 100129.
71 Z. Wang, W. Xu, Z. Wang, D. Lyu, Y. Mu, W. Duan and Y. Wang, *J. Am. Chem. Soc.*, 2021, **143**, 19881–19892.
72 X. Liu, X. Sun, Y. Peng, Y. Wang, D. Xu, W. Chen, W. Wang, X. Yan and X. Ma, *ACS Nano*, 2022, **16**, 14666–14678.
73 K. Vikrant and K.-H. Kim, *Catal. Sci. Technol.*, 2021, **11**, 6592–6600.
74 M. Falahati, M. Sharifi and T. L. M. T. Hagen, *J. Nanobiotechnol.*, 2022, **20**, 153.
75 L. Wang, H. Zhu, Y. Shi, Y. Ge, X. Feng, R. Liu, Y. Li, Y. Ma and L. Wang, *Nanoscale*, 2018, **10**, 11384–11391.
76 S. Gao, J. Hou, J. Zeng, J. J. Richardson, Z. Gu, X. Gao, D. Li, M. Gao, D.-W. Wang, P. Chen, V. Chen, K. Liang, D. Zhao and B. Kong, *Adv. Funct. Mater.*, 2019, **29**, 1808900.
77 Z. Guo, T. Wang, A. Rawal, J. Hou, Z. Cao, H. Zhang, J. Xu, Z. Gu, V. Chen and K. Liang, *Mater. Today*, 2019, **28**, 10–16.
78 A. Terzopoulou, X. Wang, X.-Z. Chen, M. Palacios-Corella, C. Pujante, J. Herrero-Martín, X.-H. Qin, J. Sort, A. J. deMello, B. J. Nelson, J. Puigmartí-Luis and S. Pané, *Adv. Healthcare Mater.*, 2020, **9**, 2001031.
79 C.-G. Liu, C.-P. Fu, Y.-H. Shi, J. Zhong, H.-X. Tang, J.-T. Zhang, R. Kumar Kankala, S.-B. Wang and A.-Z. Chen, *Mater. Des.*, 2022, **222**, 111039.
80 Y. You, D. Xu, X. Pan and X. Ma, *Appl. Mater. Today*, 2019, **16**, 508–517.
81 Z. Liu, T. Li, N. Li, Y. Wang, L. Chen, X. Tang, M. Wan and C. Mao, *Sci. China: Chem.*, 2022, **65**, 989–1002.
82 R. Wang, W. Guo, X. Li, Z. Liu, H. Liu and S. Ding, *RSC Adv.*, 2017, **7**, 42462–42467.
83 L. Chen, M.-J. Zhang, S.-Y. Zhang, L. Shi, Y.-M. Yang, Z. Liu, X.-J. Ju, R. Xie, W. Wang and L.-Y. Chu, *ACS Appl. Mater. Interfaces*, 2020, **12**, 35120–35131.
84 S. Wang, H. Ye, Y. Wang and X. Ma, *ChemistrySelect*, 2022, **7**, e202104034.
85 J. Yang, J. Li, X. Yan, Y. Lyu, N. Xing, P. Yang, P. Song and M. Zuo, *ACS Appl. Mater. Interfaces*, 2022, **14**, 6484–6498.
86 Z. Guo, J. Liu, Y. Li, J. A. McDonald, M. Y. Bin Zulkifli, S. J. Khan, L. Xie, Z. Gu, B. Kong and K. Liang, *Chem. Commun.*, 2020, **56**, 14837–14840.
87 H. Chen, H. Zhu, J. Huang and X. Feng, *J. Mater. Eng. Perform.*, 2020, **29**, 6196–6200.
88 W. Yang, Y. Qiang, M. Du, Y. Cao, Y. Wang, X. Zhang, T. Yue, J. Huang and Z. Li, *J. Hazard. Mater.*, 2022, **435**, 128967.
89 H. Huang, J. Li, M. Yuan, H. Yang, Y. Zhao, Y. Ying and S. Wang, *Angew. Chem., Int. Ed.*, 2022, **61**, e202211163.
90 W. Yang, J. Li, Z. Xu, J. Yang, Y. Liu and L. Liu, *J. Mater. Chem. C*, 2019, **7**, 10297–10308.
91 K. Wang, W. Wang, S. Pan, Y. Fu, B. Dong and H. Wang, *Appl. Mater. Today*, 2020, **19**, 100550.
92 Z. Guo, Y. Wu, Z. Xie, J. Shao, J. Liu, Y. Yao, J. Wang, Y. Shen, J. J. Gooding and K. Liang, *Angew. Chem., Int. Ed.*, 2022, **61**, e202209747.
93 R. Maria-Hormigos, B. Jurado-Sánchez and A. Escarpa, *Anal. Bioanal. Chem.*, 2022, **414**, 7035–7049.
94 Z.-Y. Gu, C.-X. Yang, N. Chang and X.-P. Yan, *Acc. Chem. Res.*, 2012, **45**, 734–745.
95 R. Rodríguez-Ramos, Á. Santana-Mayor, B. Socas Rodríguez, A. V. Herrera-Herrera and M. Á. Rodríguez Delgado, in *Metal-Organic Frameworks for Chemical Reactions*, ed. A. Khan, F. Verpoort, A. M. Asiri, M. E. Hoque, A. L. Bilgrami, M. Azam and K. C. B. Naidu, Elsevier, 2021, pp. 167–230, DOI: 10.1016/B978-0-12-822099-3.00009-5.